High-Performance Thermally Self-Cross-Linked Polymer of Intrinsic Microporosity (PIM-1) Membranes for Energy Development

ARTICLE *in* MACROMOLECULES · FEBRUARY 2012

Impact Factor: 5.8 · DOI: 10.1021/ma202667y

4 AUTHORS, INCLUDING:

Tai-Shung Chung
National University of Singapore
726 PUBLICATIONS **19,531** CITATIONS
SEE PROFILE

S. Kawi
National University of Singapore
203 PUBLICATIONS **5,439** CITATIONS
SEE PROFILE

Macromolecules

Article

pubs.acs.org/Macromolecules

High-Performance Thermally Self-Cross-Linked Polymer of Intrinsic Microporosity (PIM-1) Membranes for Energy Development

Fu Yun Li,[†] Youchang Xiao,[‡] Tai-Shung Chung,*[,†] and Sibudjing Kawi[†]

[†]Department of Chemical & Biomolecular Engineering, National University of Singapore, 4 Engineering Drive 4, 117576 Singapore

[‡]Suzhou Faith & Hope Membrane Technology Co., Ltd., Suzhou Industrial Park, Jiangsu Province, 215123, PR China

ABSTRACT: Novel thermally self-cross-linked polymers of intrinsic microporosity (PIM-1) membranes have been prepared by postmodification of PIM-1 at the elevated temperature for a period of 0.5−2 days. The occurrence of cross-linking reaction has been verified by thermogravimetric analysis (TGA), X-ray photoelectron spectrometer (XPS) and gel content analyses. TGA analyses indicate an increase in thermal stability of membranes after the thermal cross-linking treatment. There is also an obvious drop in the maximum decomposition rate comparing to the original PIM-1when membranes are thermally treated for an extended period of time. Both FTIR and XPS results suggest that the nitrile-containing PIM-1 membranes undergo a latent cross-linking reaction, and form stable bulky triazine rings. The resultant cross-linked polymeric membranes exhibit exceptional gas separation performance that surpasses the most recent upper bound of state-of-the-art polymeric membranes for the important gas separations, such as hydrogen purification, CO_2 capture and flue gas separation. In addition, both gas permeability (attributed to the contorted nature, rearrangement and pronounced inefficient packing of PIM polymer chains) and selectivity (attributed to the decrease of chain-to-chain spacing) increase diagonally with the upper bound line when thermal soaking time increases. PIM-1 thermally treated at 300 °C for 2 days has the CO_2 permeability of 4000 barrer with CO_2/CH_4 and CO_2/N_2 ideal selectivity of 54.8 and 41.7, respectively. The thermally cross-linked PIM-1 membranes will probably provide a promising alternative in industrial energy development.

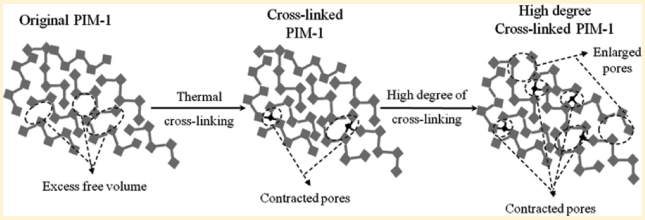

INTRODUCTION

Natural gas purification and carbon capture by membrane technology have attracted great interest in the recent years due to the simplicity, ease of scale-up and environmental friendliness of membrane processes as compared to conventional gas separation methods such as amine absorption, pressure swing adsorption or cryogenic separation.[1,2] Polymeric materials are suitable candidates for fabricating membranes owing to their low cost and ease of processability into different configurations.[3] There are many factors affecting the gas separation performance of a polymeric membrane. High permeation flux and gas-pair selectivity are regarded as two of the most important criteria for the selection of a membrane for industrial use. This is because high permeation flux is desired to minimize the membrane area required and thus reduce the production cost while high selectivity would enhance the separation efficiency and hence achieve high purity products.[4−7] Membranes fabricated from commercial polymeric materials typically have a low permeation flux. This drives researchers to develop novel materials with a higher flux. However, there exists a trade-off behavior between permeability and selectivity; namely, an increase in permeability of the more permeable gas component usually results in a decline in selectivity. This trend is depicted by the upper-bound line that Robeson has derived from many polymeric membranes.[8] Continuous research efforts have focused on developing membranes that deviate and surpass the upper bound relationship.

Recently, a novel class of polymers, termed "polymers of intrinsic microporosity" (PIMs) has emerged as a promising membrane material for gas separation.[9−17] It possesses unusually high free volume and high surface areas (i.e., ~700 $m^2\ g^{-1}$ for PIM-1), which can be mainly ascribed to its special ladder-type structures with contorted sites that prevent rotation of polymer chains and efficient space packing. Besides their high surface areas, PIMs also exhibit easy solution processability with a high degree of microporosity. Among all the PIMs synthesized, PIM-1 is one of the most well-known types for membrane gas separation.[16,17] The pristine PIM-1 membrane has demonstrated extremely high gas permeability with moderate-to-good separation factor for several important gas pairs (e.g., O_2/N_2, CO_2/N_2, and CO_2/CH_4).[10,13] Later on, several works have attempted to postmodify the PIM-1 membrane to further enhance its gas transport properties mainly with respect to gas-pair selectivity.

In the work of Du et al.,[18] the nitrile groups of PIM-1 were converted to carboxyl groups via a simple postmodification hydrolysis reaction. The degree of conversion could be controlled by the hydrolysis time and temperature. In terms of gas permeation separation performance, the hydrolyzed PIM-1 membranes revealed an evident decrease in gas

Received: December 8, 2011
Revised: January 20, 2012
Published: January 31, 2012

permeability and obvious increase in gas-pair selectivity. However, the overall gas separation performance still followed the upper bound line in which an increase in gas-pair selectivity was at the expense of gas permeability. The researchers at UOP[19] proposed a UV-cross-linking approach to possibly tighten the polymer chains and reduce the interchain space for gas separation. The PIM-1 membrane under UV-cross-linking treatment for a period of 30 min exhibited O_2/N_2 selectivity of 5.4 with O_2 permeability of 147 barrer. However, no detailed scientific explanation was disclosed in this work. Recently, Du et al.[20] incorporated CO_2-philic pendant tetrazole groups into PIM-1 membranes and the resultant membranes revealed an obvious enhancement in gas permeation separation performance. It provided a viable alternative for CO_2 capture from flue gas. In another work done by Mason et al.,[21] they converted the original nitrile group to the thioamide groups in PIM-1 by using phosphorus pentasulfide as the thionating agent. The modified thioamide-PIM-1 membrane showed an increased selectivity but a reduced permeability compared to the pristine PIM-1 membrane.

In order to enhance the gas-pair selectivity and at the same time maintaining the gas permeability of PIM-1 membranes, we sought to molecularly design the cavity size of PIM-1 membrane by the cross-linking method. In this work, we report the preparation of thermally self-cross-linked PIM-1 membranes via the inherent cross-linking reaction of aromatic nitrile groups to form triazine rings at the elevated temperature with a prolonged treatment time. It is worthwhile to note that the bulky triazine rings formed in the polymer matrix might induce inefficient packing of polymer chains such that the expected decrease in gas permeability due to the cross-linking reaction may be minimized. The thermal cross-linking reaction of the nitrile containing polymers has been well documented in the literatures.[22−26] The cross-linking reaction could be either carried out at elevated temperatures with a prolonged thermal treatment time[22−24] or catalyzed at a lower temperature.[23,25,26] The detailed synthesis method and characterizations of PIM-1 polymer are reported in this work to ensure the correct base material has been used in this study. The effects of thermal cross-linking temperature and duration on gas separation properties of PIM-1 membranes have been investigated and compared with the Robeson's upper bounds.

EXPERIMENTAL SECTION

Materials. 5,5′,6,6′-Tetrahydroxy-3,3,3′,3′-tetramethyl-1,1′-spirobisindane (TTSBI, 97%) purchased from Alfa Aesar, was recrystallized from methanol. 2,3,5,6-tetrafluoroterephthalonitrile (TFTPN, 99%) supplied by Sigma-Aldrich, was sublimated under vacuum prior to use. Anhydrous potassium carbonate (K_2CO_3, ≥ 99%) from Sigma-Aldrich, methanol (MeOH, ≥ 99.9%) from Merck and HPLC grade tetrahydrofuran (THF, 99.9%) from Fisher Chemical, were used as received. Dichloromethane (DCM, 99.99%) and hydrochloric acid (HCl, 37.5%) were obtained from Fisher Scientific and also used as received. *N*-Methyl-2-pyrrolidone (NMP, > 99.5%) from Merck was further purified via distillation prior to use.

Synthesis of PIM-1. The synthesis of PIM-1 is based on polycondensation of TFTPN with TTSBI.[9,15] A stoichiometric amount of anhydrous K_2CO_3 was added to a mixture consisting of equimolar amounts of TFTPN and TTSBI dissolved in NMP under a nitrogen atmosphere with vigorous stirring. After 30 min of nitrogen purging to remove air and moisture, the reaction solution was immersed into a preheated 60 °C oil bath for 24 h. Upon cooling, the mixture was added to MeOH and the crude product was collected by filtration. The crude product was then washed with 0.1 wt % HCl at 70 °C for at least 2 h. The fluorescent yellow solid was filtered off and washed with fresh water until the solution was neutral. It was then washed with MeOH, dissolved in DCM, reprecipitated from MeOH again and vacuum-dried at 120 °C for at least 24 h, yield of approximately 87% was obtained. Surface area (N_2 adsorption, BET analysis): 726.4 m^2 g^{-1}. ^{1}H NMR (400 MHz, $CDCl_3$-d_6, δ): 1.2−1.4 (br. m, 12H; CH_3), 2.1−2.4 (br. m, 4H; CH_2), 6.4 (br. s, 2H; CH), 6.8 (br. s, 2H; CH). ^{13}C NMR (100 MHz, $CDCl_3$, δ): 109.4 (−CN). ^{19}F NMR (376 MHz, $CDCl_3$, δ): 0 (F). FTIR (ATR): 2237 cm^{-1} (−CN), 2800−3000 cm^{-1} (H−C−H); Anal. Calcd (XPS elemental analysis) for PIM-1 ($C_{29}H_{20}N_4O_2$): C, 79.10; N, 6.36; O, 14.54. Found: C, 79.23; N, 6.20; O, 14.57.

Dense Membrane Preparation. A 2% (w/w) of polymer solution was prepared by dissolving readily soluble PIM-1 powder in DCM. The polymer solution was filtered using a 1.0 μm Whatman's filter before ring casting onto a silicon wafer plate at room temperature (i.e., 25 ± 2 °C) to allow slow evaporation of the solvent. Dense membranes were formed after approximately 5 days. The nascent dense films were then soaked in MeOH to remove prior membrane formation history and any residual possible solvents and dried in a vacuum oven at 120 °C to remove the residual solvent. Membranes with the thickness of 55 ± 5 μm were used for further studies.

Thermal Cross-Linking Treatments. The thermal cross-linking treatments of PIM-1 dense films were performed using a Centurion Neytech Qex vacuum furnace. The vacuum furnace temperature was raised to between 250 and 300 °C at a rate of 10 °C/min and held for a period of 0.5 to 2 days. After the thermal cross-linking treatment process, the membranes were cooled naturally in the vacuum furnace to room temperature and stored in a drybox for further studies. A clear coloration from yellow to dark brown and black color could be observed for the thermal-treated membranes depending on the duration and temperature of thermal treatments. In addition, all membranes after thermal treatments were flexible and tough enough for characterization and gas permeation measurements. The weights before and after the thermal treatment process of each membrane were measured and no obvious weight loss was observed (i.e., <2 wt %). The membrane dense films were labeled as "PIM-temperature-duration (day)", for example, PIM-300−0.5d.

Characterizations. The molecular weight of the synthesized PIM-1 was determined by gel-permeation chromatography (GPC) measurements. It was carried out on a HP 1100 HPLC system equipped with the HP 1047A RI detector and Agilent 79911GP-MXC columns. THF was used as the solvent and the flow rate was controlled at 1.0 mL/min. The PIM-1 powder was dissolved in THF at a concentration of 0.005 wt %. The molecular weight was estimated by comparing the retention times in the column to those of polystyrene standards. The obtained GPC result for PIM-1 is as follows: M_n: 39828. M_w: 66674. PDI (=M_w/M_n): 1.67.

The gel content of the cross-linked PIM-1 membranes with respect to the cross-linking duration at 300 °C was determined by soaking the respective membranes into DCM solvent for 24 h. The remaining insoluble portions of the membranes were dried under vacuum at 120 °C for 24 h to remove residual solvent before weighing. The gel content was evaluated using eq 1

$$\%\ \text{gel content} = M_1/M_0 \times 100 \quad (1)$$

where M_0 and M_1 are the weights of the cross-linked membrane before and after soaking in DCM, respectively.

The thermal degradation of the original PIM-1 and thermally cross-linked PIM-1 membranes were monitored by thermogravimetric analysis (TGA) with a TGA 2050 themogravimetric Analyzer (TA Instruments). The analyses were carried out with a ramping rate of 10 °C/min at temperatures ranging from 50 to 800 °C. Nitrogen was used as the purge gas and its flow rate was controlled at 50 mL/min.

The FFV of the original PIM-1 and the thermally cross-linked PIM-1 membranes were calculated based on the Bondi's method using eq 2:

$$\text{FFV} = \frac{V - V_o}{V} \quad (2)$$

where V is the specific volume of the polymer calculated from the measured density. V_o is the volume occupied by the polymer molecules and equals to 1.3 times of the polymer's van der Waals volume (V_w). The estimation of van der Waals volume was based on the group contribution method.

The possible structural change before and after the thermal cross-linking process has been monitored by FTIR analyses. The FTIR measurements were performed using an attenuated total reflection mode (FTIR-ATR) with a Perkin-Elmer Spectrum 2000 FTIR spectrometer. Each sample was scanned 32 times. The characteristic band at 2350 cm^{-1} is contributed from carbon dioxide.

An X-ray photoelectron spectrometer (XPS) was utilized to monitor the chemical changes of thermally cross-linked PIM-1 membranes. They were carried out on an AXIS HSi spectrometer (Kratos Analytical Ltd., England) using a monochromatic Al Kα X-ray source (1486.6 eV photons) at a constant dwell time of 100 ms and a pass energy of 40 eV under full vacuum. The anode voltage and anode current were 15 kV and 10 mA, respectively. All core-level spectra were obtained at a photoelectron takeoff angle of 90 owith respect to the sample.

The positron annihilation lifetime (PAL) experiments were conducted for both the original PIM-1 and the thermally cross-linked PIM-1 membranes using a variable-energy positron beam with a counting rate of 100−500 counts/s and each spectrum contains one million counts. In PAL measurements, the quantitative information on free-volume size, distribution and content is mainly ascribed to so-called the pick-off annihilation of long-lived orthopositronium (o-Ps, the triplet bound state of a positron and an electron).[27] The estimated pick-off lifetime of the o-Ps (τ_3 in ns) is correlated to the mean free volume radius R (Å) by a semiempirical spherical-cavity model as follows:[27,28]

$$\tau_3^{-1} = 2\left[1 - \frac{R}{R_o} + \frac{1}{2\pi}\sin\left(\frac{2\pi R}{R_o}\right)\right] \tag{3}$$

Here R_o is the infinite spherical potential radius that is equal to $R + \Delta R$ with ΔR as an empirical parameter (= 1.66 Å). The relative fractional free volume (FFV) is calculated based on the Williams−Landel−Ferry (WFL) equation[29]

$$\mathrm{FFV} = 0.0018 I_3 \langle v_f(\tau_3)\rangle = 0.0018 I_3\left(\frac{4}{3}\pi R^3\right) \tag{4}$$

where I_3 is the o-Ps intensity (in %) for the estimated pick-off lifetime τ_3 and v_f is the mean free volume (in Å^3) of a cavity in the polymer matrix calculated based on the mean free volume radius R. The obtained PAL data were fitted into three lifetimes using the PATFIT program, which assumes a Gaussian distribution of the logarithm of the lifetime for each component. The MELT program was also adopted to observe the trend for free volume distribution of various membranes. A detailed description of PAL can be obtained elsewhere.[27−31]

Measurement of Gas Transport Properties. The host and thermally cross-linked PIM-1 dense membranes were tested in both pure gas and mixed gas systems. The pure gas permeation properties were evaluated by a variable-pressure constant-volume method. The detailed experimental design and procedures can be found elsewhere.[32] Each pure gas was tested in the sequence of H_2, O_2, N_2, CH_4, and CO_2 at 35 °C and 3.5 atm. The rate of pressure increase (dp/dt) at steady state was used for the calculation of gas permeability with accordance to the following eq:

$$P = \frac{273.15 \times 10^{10}}{760}\frac{Vl}{AT(P_2 \times 76/14.7)}\left(\frac{dp}{dt}\right) \tag{5}$$

where P is the gas permeability of a membrane in Barrer (1 barrer = 1×10^{-10} cm^3 (STP)-cm/cm^2s cmHg), V is the volume of the downstream chamber (cm^3), l is the membrane thickness (cm), A refers to the effective area of the membrane (cm^2), T is the operating temperature (K) and P_2 is the upstream operating pressure (psia).

The ideal selectivity of a membrane for pure gases A to B is defined as follows:

$$\alpha_{A/B} = \frac{P_A}{P_B} \tag{6}$$

where P_A and P_B are the pure gas permeability of gases A and B, respectively.

The mixed gas permeation properties for a selected cross-linked PIM-1 membrane were obtained from a modified pure gas permeation cell. The detailed experimental design and procedures can be found in the work of Tin et al.[33] Both CO_2/CH_4 mixture (50%/50% mole fraction) and CO_2/N_2 mixture (50%/50% mole fractions) were used in mixed gas tests and they were carried out at 35 °C and 7 atm. The gas permeability was evaluated as follows:

$$P_a = \frac{273.15 \times 10^{10}}{760}\frac{y_a Vl}{AT(76/14.7)(x_a P_2)}\left(\frac{dp}{dt}\right) \tag{7}$$

$$P_b = \frac{273.15 \times 10^{10}}{760}\frac{(1 - y_a)Vl}{AT(76/14.7)[(1 - x_a)P_2]}\left(\frac{dp}{dt}\right) \tag{8}$$

Here x_a is the mole fraction of gas component a in the feed gas and y_a denotes the mole fraction of gas component a in the permeate. All the other symbols remain the same meanings as described previously.

The selectivity of the mixed gas was evaluated by taking the ratio of permeate (y) and feed (x) mole fraction of two components with the following eq:

$$\alpha_{a/b} = \frac{y_a/y_b}{x_a/x_b} \tag{9}$$

The physical aging behavior of the original PIM-1 membrane and the thermally cross-linked PIM-1 membrane (i.e., PIM-300−2.0d) were preliminarily studied through a period of 240 h. H_2, O_2, N_2 and CH_4 were used in the aging test except CO_2 due to its high solubility in glassy polymers that may alter the nature of the glassy state. All membranes used in the aging study had a thickness of 55 ± 5 μm.

RESULTS AND DISCUSSION

Characterization of the Thermally Cross-Linked PIM-1 Membranes. The thermal stabilities of the original PIM-1 and the thermally cross-linked PIM-1 membranes were monitored by TGA and their degradation curves are depicted in Figure 1. As can be seen, all membranes are thermally stable up to 450 °C possibly due to the strong dipolar interactions of nitrile groups.[12] If the thermal degradation temperature is defined as a 5 wt % loss of the original weight, the longer thermal-treated PIM-1 membranes (i.e., PIM-300−1.5d and PIM-300−2d) tend to decompose at a rather later stage, which is mainly attributed to the high degree of thermal cross-linking, that stabilizes the membrane structure. Moreover, the original PIM-1 membrane exhibits the highest decomposition rate (i.e., 0.822 wt%/°C) when it starts to decompose, whereas the maximum decomposition rates of the thermally cross-linked PIM-1 membranes descend with an increase in thermal treatment time. For example, there is a clear decrease in the maximum decomposition rate from 0.822 to 0.145 wt %/°C for the original PIM-1 and the PIM-300−2d membranes, respectively. Thus, the thermally cross-linked PIM-1 membranes demonstrate much slower thermal decomposition rate when compared to the original PIM-1 membrane. Additionally, the cross-linked PIM-1 membranes show much higher weight retentions at 600 °C, which is the result of greatly enhanced thermal stability after the thermal cross-linking reaction. It is worth pointing out that all membranes contain a char yield of

dx.doi.org/10.1021/ma202667y | Macromolecules 2012, 45, 1427−1437

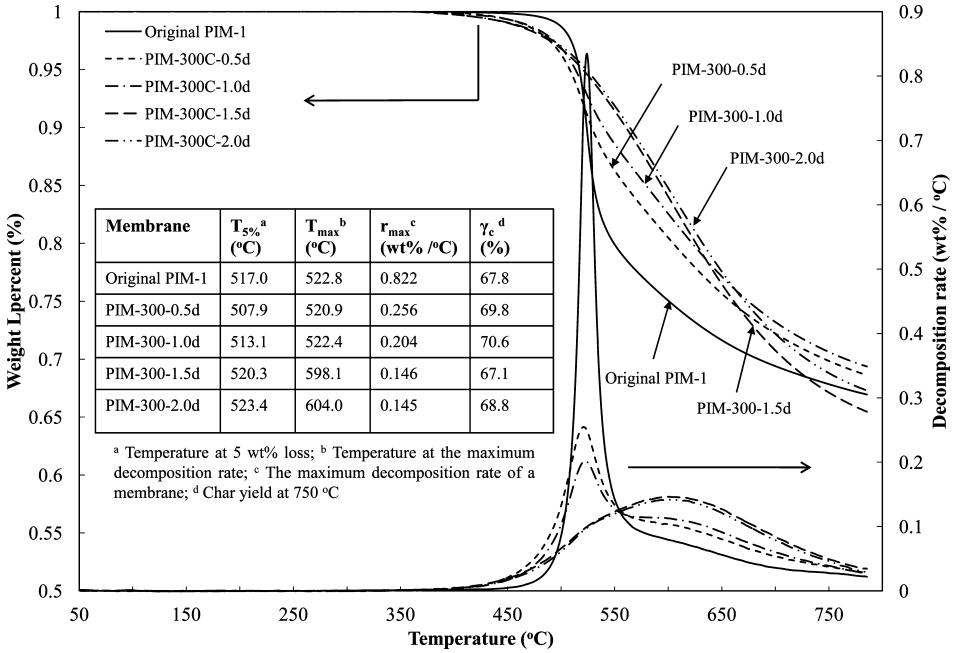

Membrane	$T_{5\%}$ [a] (°C)	T_{max} [b] (°C)	r_{max} [c] (wt% /°C)	γ_c [d] (%)
Original PIM-1	517.0	522.8	0.822	67.8
PIM-300-0.5d	507.9	520.9	0.256	69.8
PIM-300-1.0d	513.1	522.4	0.204	70.6
PIM-300-1.5d	520.3	598.1	0.146	67.1
PIM-300-2.0d	523.4	604.0	0.145	68.8

[a] Temperature at 5 wt% loss; [b] Temperature at the maximum decomposition rate; [c] The maximum decomposition rate of a membrane; [d] Char yield at 750 °C

Figure 1. TGA of the original and the thermally cross-linked PIM-1 membranes.

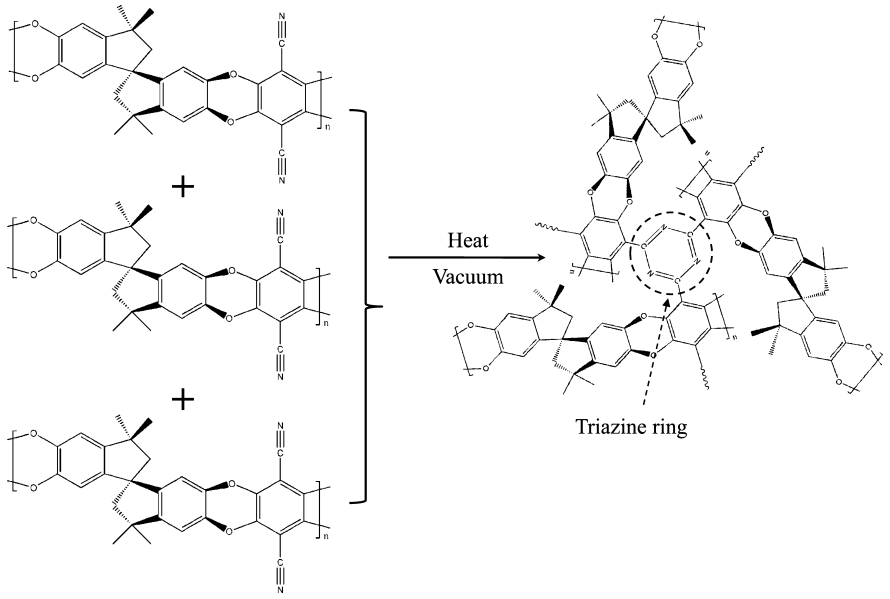

Figure 2. Proposed thermal cross-linking reaction of PIM-1.[22−24]

more than 65 wt % at 750 °C due to the unusual thermal stability of the intrinsic microporosity material.

A good indication of the occurrence and the extent of cross-linking reaction at the respective thermal treatment duration are provided by the gel content of the modified films. It is observed that there is about 86% gel content for PIM-300−0.5d, while no obvious weight loss (e.g., approximately 100% gel content) could be detected when the PIM-1 membranes are treated more than 0.5 d at 300 °C. The results from gel content reinforce the confirmation of cross-linked structure of PIM-1 membranes. It also suggests that the extent of cross-linking reaction increases with thermal treatment time.

Although both TGA and Gel content analyses demonstrate the occurrence of thermal cross-linking reaction, it is hard to know their exact chemical structure because there are many possible structures deriving from the possibly activated cyano groups.[26] According to literatures, the most likely chemical cross-linking reaction scheme is having a thermally induced trimerization of the nitriles to stable triazine rings without releasing any volatile side products, as shown in Figure 2.[22−24] However, the thermal trimerization process is slow and might be expedited by either catalyst or conducting at elevated temperature with an extended period of time.[24,25] The structural changes and the formation of triazine structures of the thermally treated PIM-1 membranes have been verified by FTIR and XPS analyses.

Figure 3 depicts the FTIR spectra for the original and the selected thermally cross-linked PIM-1 films. The FTIR spectrum of PIM-300−2.0d membrane is not showing here due to its relatively weak IR signal. This is probably caused by

dx.doi.org/10.1021/ma202667y | Macromolecules 2012, 45, 1427−1437

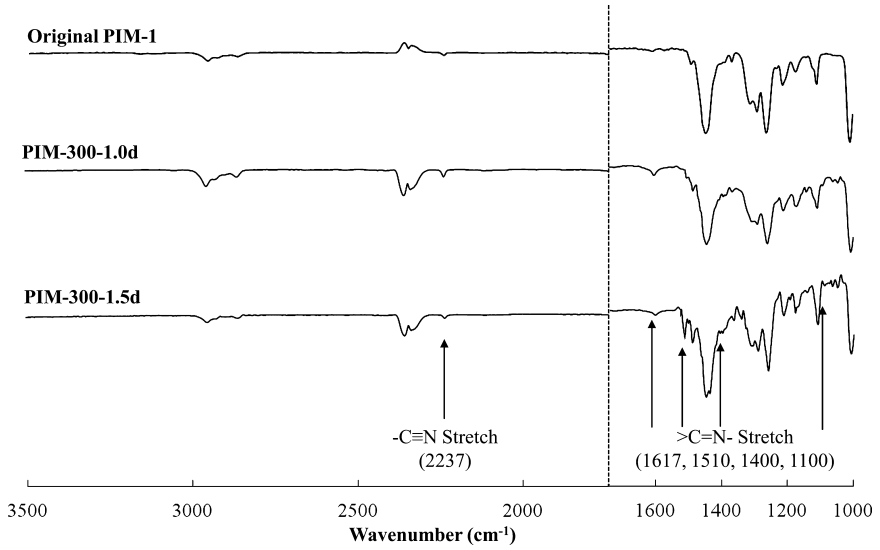

Figure 3. FTIR spectra of the original and the thermally cross-linked PIM-1 membranes.

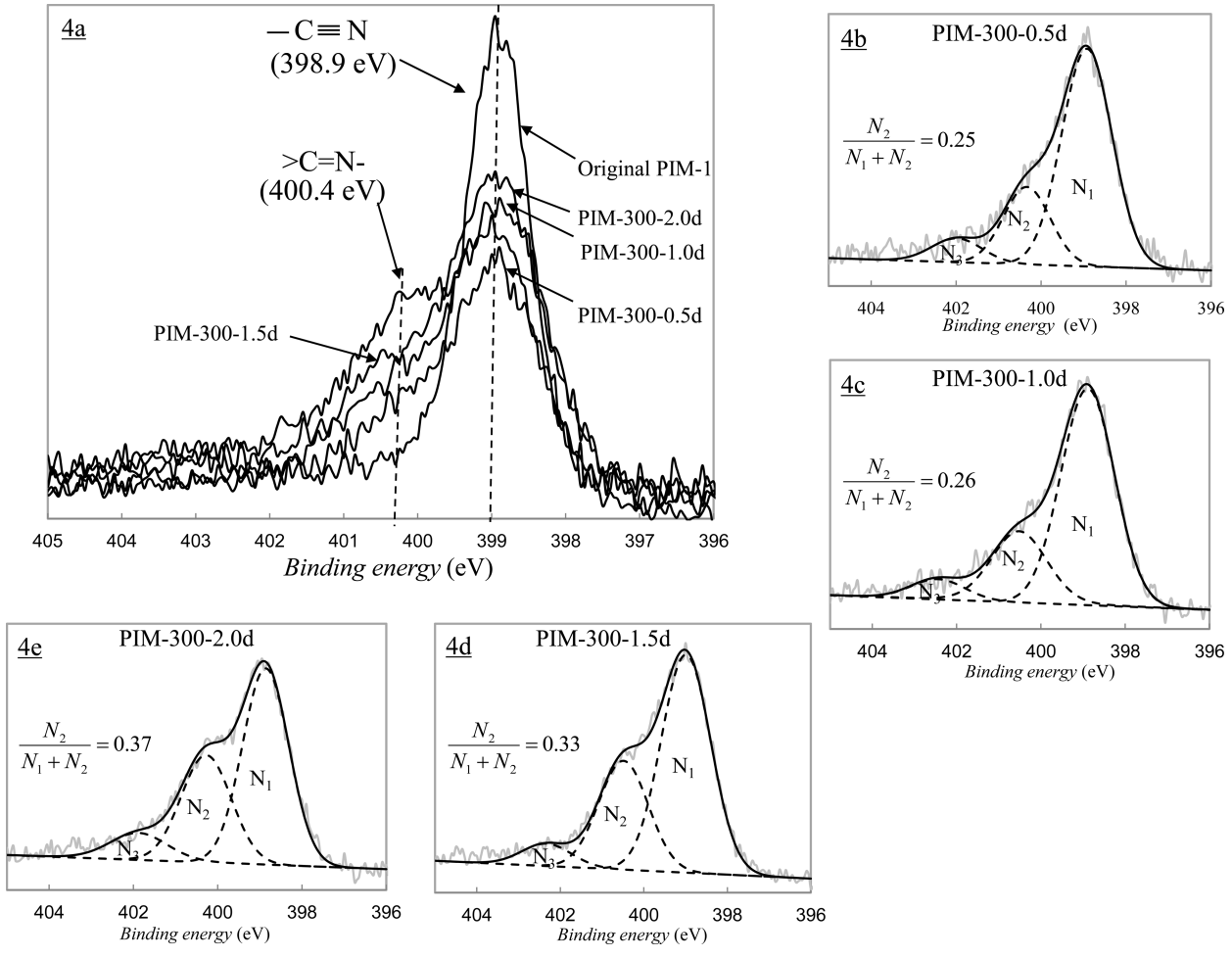

Figure 4. N_{1s} XPS analysis of the original and the thermally cross-linked PIM-1 membranes.

the weak IR reflection since this membrane is a bit dark in color. The prominent peak at 2237 cm^{-1} is attributed to the −C≡N stretching. Comparing with the original PIM-1 film, there are a few distinct new peaks near 1617, 1510, 1400, and 1100 cm^{-1}, which are characteristic peaks of >C═N− stretching and bending vibrations.[26,34] This, on the other hand, confirms the formation of triazine structure after the thermal cross-linking process. Besides, XPS analyses have been used to determine the extent of thermal cross-linking process.

Figure 4 shows the N_{1s} XPS spectrum of the host PIM-1 and the thermally cross-linked PIM-1 membranes. The original PIM-1 membrane reveals a symmetrical Gaussian-type N_{1s} core

dx.doi.org/10.1021/ma202667y | Macromolecules 2012, 45, 1427−1437

Table 1. Pure Gas Separation Performance of the Original and the Thermally Cross-Linked PIM-1 Membranes (Tested at 35 °C and 3.5 atm)

	permeability (Barrer[a])					ideal selectivity				
membranes	H_2	O_2	N_2	CH_4	CO_2	H_2/N_2	H_2/CH_4	O_2/N_2	CO_2/CH_4	CO_2/N_2
pristine PIM-1	2696	712	166	204	3375	16.3	11.7	4.3	16.6	20.4
original PIM-1[b]	3949	1257	337	472	6957	11.7	8.4	3.7	14.8	20.7
PIM-250−1.0d	1430	400	107	145	2220	13.3	9.9	3.7	15.3	20.7
PIM-250−2.0d	1360	326	76	73	1968	17.9	18.6	4.3	27.0	25.9
PIM-300−0.5d	1666	422	99	97	2496	16.9	17.2	4.3	25.9	25.3
PIM-300−1.0d	2221	483	101	91	3083	22.1	24.5	4.8	34.0	30.7
PIM-300−1.5d	2640	557	106	95	3339	24.9	31.1	5.2	39.3	31.4
PIM-300−2.0d	3872	582	96	73	4000	40.3	53.0	6.1	54.8	41.7

[a]1 barrer =1 × 10^{-10} cm^3(STP)cm/cm^2 s cmHg. [b]Soaked in MeOH.

signal with the maximum peak at 398.9 eV which is ascribed to the −C≡N (nitrile) group in the PIM-1 polymer structure. After the thermal treatments, the symmetrical N_{1s} core signal becomes broad and asymmetrical with newly formed shoulder peaks at about 400.4 eV, which belong to the nitrogen of the >C═N− (imine) group.[35−37] A positive shift of 1.5 eV of the N_{1s} core signal is consistent with a loss of a negative charge in the nitrogen of the >C═N− group from the −C≡N group.[35,36] The partial conversion of the original nitrile group in the PIM-1 structure to the imine group is indeed caused by the thermally induced cross-linking reaction of the polymer chains.

In order to quantitatively monitor the extent of cross-linking reaction, the N_{1s} XPS spectrum of each cross-linked PIM-1 membrane was deconvoluted into three peaks at 398.9, 400.4, and 402.2 eV with a fixed fwhm of 1.4 eV. The highest decomposed N_{1s} binding energy of 402.2 eV is probably attributed to the π-excitation which appears in all carbon compounds with double bonds.[38] As illustrated in Figure 4b−e, the ratio of integrated intensity >C═N−/(>C═N− + −C≡N) (i.e., $N_2/(N_1 + N_2)$) shows an increasing trend with an increase in thermal treatment time, which suggests that the extent of thermal cross-linking is more pronounced at an extended duration of thermal treatment. For example, the conversion rate of -C≡N to the triazine structure for PIM-300−0.5d is 25%, whereas, the conversion has increased to 37% when the membrane is soaked at 300 °C for 2 d. However, thermal-treating of PIM-1 for more than 2 d would lead to the subtle brittleness of the treated membranes, hence leading to difficulties in characterization and permeation test. We therefore did not continue longer thermal treatments.

A close look at the resultant cross-linked PIM-1 membranes supports the existence of cross-linking reaction. As the cross-linking duration increases, the PIM-1 membranes turn from originally yellow, to dark brown and then black in color. The coloration of cross-linked PIM-1 membranes is mainly attributed to the formation of charge-transfer complexes (CTCs) between the PIM-1 chains that having the newly formed triazine ring as the electron acceptor and benzene rings of PIM-1 as the electron donors. During the cross-linking reaction, the formation of triazine rings tends to pull the PIM-1 benzene rings approach each other closely enough to allow transfer of π−electrons, and thus generates colors.[39,40]

Pure Gas Transport Properties. The pure gas separation performance of the original and the thermally cross-linked PIM-1 membranes is shown in Table 1. As can be seen, the gas permeability of PIM-1 post-treated with methanol (i.e., original PIM-1) has increased almost 2-fold from the pristine PIM-1. Swelling might be one of the main reasons contributing to this effect.[12,13,17] A similar phenomenon has been reported by Tin et al. and Shao et al. on Matrimid and other 6FDA polyimide.[33,41,42] The original PIM-1 membrane exhibits extremely high gas permeability and moderate selectivity for all gases, which is consistent with previously reported results.[13,16,17] After 1 d thermal treatment at 250 °C under vacuum, the gas permeability for all gases decreases significantly, whereas no enhancement in gas-pair selectivity could be obtained. This is probably attributed to the mere densification of high free volume PIM-1 membrane structure at 250 °C as no cross-linking has occurred at this stage. In fact, the N_{1s} XPS spectra for PIM-250−1d (not shown here) also reveal a symmetrical Gaussian-type signal with the maximum peak at 398.9 eV, which is exactly the same as have been observed in the original PIM-1 XPS spectrum (i.e., Figure 4). As discussed previously, the thermally induced trimerization process is slow and is probably initiated at elevated temperatures with an extended period of time. The PIM-1 membrane treated at an extended duration (e.g., PIM-250−2d) reveals a further decrease in gas permeability, but a significant enhancement in gas-pair selectivity. For example, the permeability of CO_2 decreases by about 11% with an increase of 76% in CO_2/CH_4 selectivity from membrane PIM-250−1d to PIM-250−2d. This indicates that the thermal cross-linking has probably occurred at an extended duration of thermal treatment.

To further study the thermally induced trimerization process of PIM-1 membranes, the thermal cross-linking temperature was raised to 300 °C and held for a period of 0.5 to 2 d. The gas-pair selectivity of the thermally cross-linked PIM-1 membranes increases monotonically with the increase of thermal treatment time. In particular, the selectivity of CO_2/CH_4 is almost four times higher than the original PIM-1 membrane. This monotonic increase in gas-pair selectivity is mainly attributed to the thermally induced cross-linking of polymer chains that tightens polymer chains of PIM-1. The possible tightening of polymer chains with an increase in thermal treatment time has been verified by PAL experiments. Table 2 shows the PAL results of the original and the thermal-treated PIM-1 membranes under different thermal soaking durations. Generally, an increase in thermal soaking time of PIM-1 membranes decreases the τ_3 value. To be exact, this could be caused by either the physical densification of membrane structure at elevated temperatures or the chemical tightening of polymer chains due to the formation of triazine rings within the PIM-1 matrix. However, the N_{1s} XPS results indicate that the extent of thermal cross-linking increases with soaking time when the soaking temperature is fixed at 300 °C.

dx.doi.org/10.1021/ma202667y | Macromolecules 2012, 45, 1427−1437

Table 2. PAL Results of the Original and the Thermally Cross-Linked PIM-1 Membranes

membranes	τ_3 (ns)	I_3 (%)	R_3 (Å)	FFV(%)	FFV (%)[a]
original PIM-1[b]	3.08 ± 0.07	13.82 ± 0.34	3.69 ± 0.03	5.24 ± 0.26	23.9 ± 0.4
PIM-300−0.5d	2.79 ± 0.07	13.11 ± 0.50	3.49 ± 0.04	4.20 ± 0.29	16.1 ± 0.6
PIM-300−1.0d	2.59 ± 0.05	11.13 ± 0.26	3.36 ± 0.03	3.18 ± 0.16	15.9 ± 0.5
PIM-300−1.5d	2.52 ± 0.09	10.48 ± 0.64	3.29 ± 0.05	2.82 ± 0.31	16.6 ± 0.4
PIM-300−2.0d	2.44 ± 0.08	11.43 ± 0.58	3.23 ± 0.05	2.90 ± 0.27	17.1 ± 0.4

[a]Calculated based on Bondi's method. [b]Soaked in MeOH.

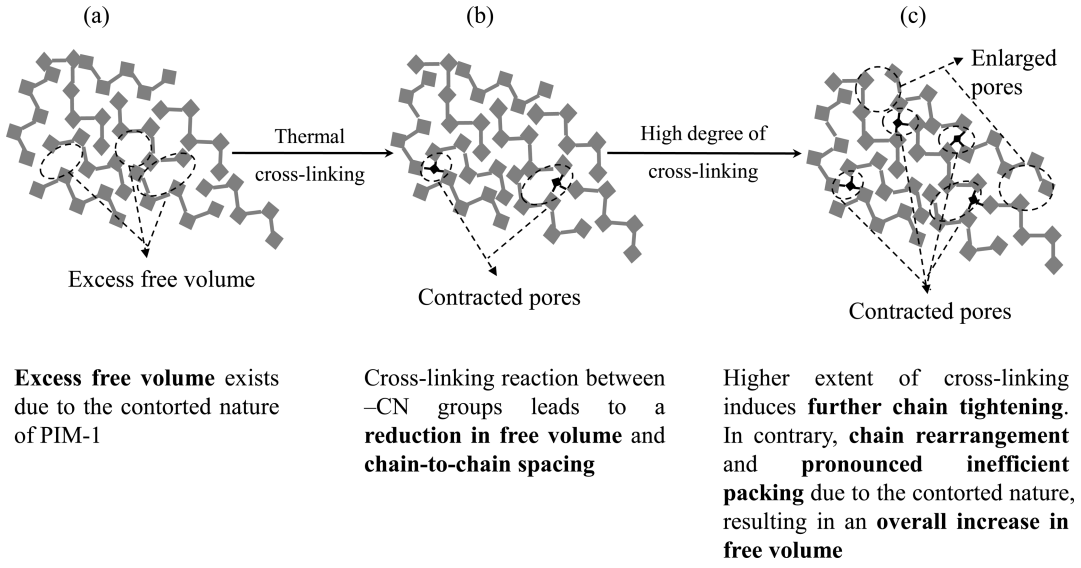

Figure 5. Two-dimensional representations of the contorted PIM-1 membrane before and after thermal cross-linking reaction with the formation of triazine rings. (a) Original PIM-1 matrix (time = 0). (b) Initiation of thermal cross-linking process (time ≫ 0). (c) Completion of thermal cross-linking process (time ≫ 0).

Hence, the decrease in o-Ps lifetime (i.e., τ_3 or corresponding mean pore size r_3) is mainly resulted from the tightening of polymer chains during the cross-linking process. A comparison between the original PIM-1and the thermal-treated PIM-300−2d membrane sees a decrease of τ_3 from 3.08 to 2.44 ns while the corresponding r_3 dwindles from 3.69 to 3.23 Å.

Generally, the calculated fractional free volume (FFV) based on τ_3 value also indicates a decrease for the thermally cross-linked PIM-1 membranes when compared to the original PIM-1 membrane. One possible reason is due to the fact that the cross-linking reaction tightens polymer chains, thereby resulting in a lower free volume. It is worthwhile to point out that the PAL calculated FFV of PIM-1 membranes is smaller than the FFV calculated based on the Bondi's method, and the calculated FFV of PIM-1 based on the Bondi's method is consistent with previously reported results.[12,14] This is because PAL experiments only consider ultrafine micropores (i.e., <4 ns in τ_3 value), while Bondi's method takes consideration of all functional groups in PIM-1 polymer structures. In fact, the long lifetimes (i.e., >4 ns in τ_4 value) of PIM-1 membranes were also observed in PAL experiments. However, due to the nature of slow positron beam, the long lifetimes of o-Ps observed results from both the positron beam itself and the large micropores in the PIM-1 membranes. To reduce complexity, only three lifetimes were adopted without consideration of long lifetimes of τ_4 value.

It has been verified that there are two kinds of pores in PIM-1 based materials: large micropores and ultrafine micropores.[12,14,43] The former is mainly attributed to the loosely packed polymer chains due to the kinked structure of PIMs, while the latter is the chain-to-chain distance of space-efficiently packed polymer chains. Generally, the loosely packed polymer chains create a large free volume in the membrane and contribute mostly to the high gas permeability, whereas the chain-to-chain spacing plays a determining role in gas-pair selectivity. With the occurrence of cross-linking reaction and formation of the bulky triazine ring with the planar structure, a synergistic effect for high permeability and high selectivity is created at one step resulting from a decrease in chain-to-chain spacing at one end of the polymer chain and an increased inefficiency of chain packing at the other end, which could be envisaged with a two-dimensional schematic illustration depicted in Figure 5.

Referring to Figure 5a, the original PIM-1 polymer chains tend to pack inefficiently due to the contorted nature of PIM backbone, which in turn generates excess free volumes. When the thermal cross-linking reaction initiates, the formation of bulky planar triazine rings tends to pull the polymer chains closer to each other at one end (i.e., site of nitrile groups) as shown in Figure 2, thus resulting in an overall decrease in FFV (e.g., Figure 5b) when compared to the host PIM-1 matrix. Additionally, the cross-linking reaction leads to a decrease in chain-to-chain spacing (i.e., verified by decreasing the τ_3 value in PAL experiments), hence increasing the gas-pair selectivity. As the cross-linking reaction continues, more bulky planar triazine rings would be formed and possibly lead to the rearrangement of polymer chains. However, due to the nature of PIM materials that do not possess rotational freedom along

dx.doi.org/10.1021/ma202667y | Macromolecules 2012, 45, 1427−1437

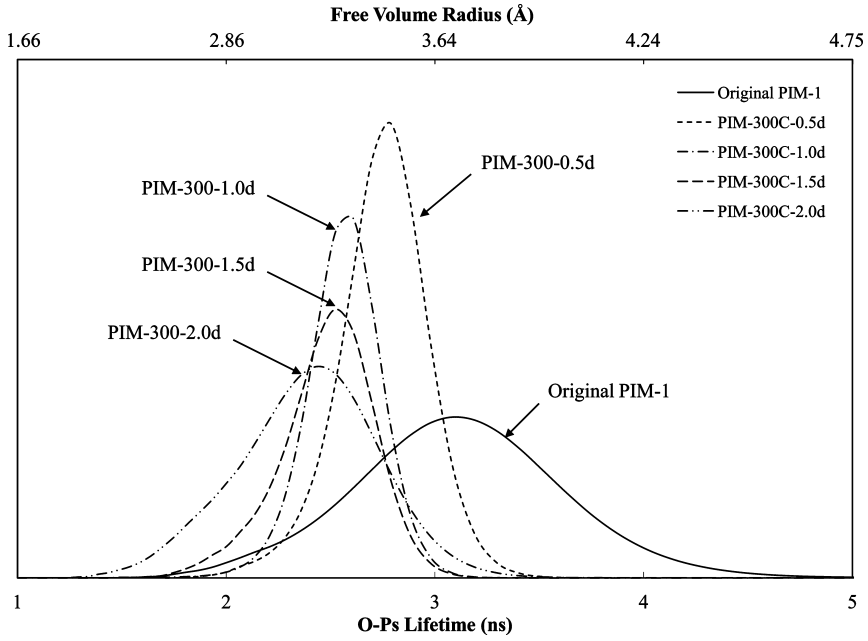

Figure 6. PAL analysis of the original and the thermally cross-linked PIM-1 membranes.

the polymer backbone,[44] the formation of bulky planar triazine rings would further constrain the movement of those polymer chains (e.g., Figure 5c). Eventually, it would induce pronounced inefficient packing, thus increases free volume and enhances gas permeability with an increase in thermal soaking duration. This is somewhat explained by the PAL data as well. As can be seen from the Table 2, there is an obvious increase in o-Ps intensity (i.e., I_3 from PAL experiments) when the PIM-1 membrane is thermally treated for a longer period of time. Although the thermal cross-linking reaction induces obvious reduction in chain-to-chain spacing, the overall FFV, which takes consideration of both τ_3 and I_3, still reveals an increase in PIM-300−2d membrane when compared to the membrane treated at a shorter period of time (i.e., PIM-300−1.5d).

To have a clearer picture of the pore size and free volume change of the thermally cross-linked PIM-1 membranes, the MELT analysis was utilized and the result is depicted in Figure 6. An increase in thermal cross-linking duration clearly shifts the peak to the left and a relatively narrower distribution is also observed. However, as the thermal cross-linking duration increases, the free volume distribution becomes broader, which suggests the various sizes of small pores have been generated when membrane is thermally treated for a longer period of time, thus the possibly more free volume and enhanced gas permeability. This is in agreement with the trend of decreasing τ_3 and increasing I_3 concluded from PATFIT results. Therefore, an effective manipulation of free volume and pore size of the PIM-1 membranes can be achieved via the thermal cross-linking reaction at the elevated temperature with an appropriate thermal soaking time. The revolution of free volume and pore size distributions toward left or become narrow indicates the thermally treated PIM-1 membranes may have higher selectivity for specific gas pair separations.

Mixed Gas Tests and Potential Applications of Thermally Cross-Linked PIM-1 Membranes. Binary CO_2/CH_4 and CO_2/N_2 tests were conducted for PIM-300−2.0d membrane at 35 °C and results are shown in Table 3. Generally, the gas permeability in mixed gas tests is lower than

Table 3. Mixed Gas Separation Performance of the Thermally Cross-Linked PIM-1 Membrane PIM-300-2.0d (Tested at 35 °C and 7.0 atm)

	permeability (Barrer[a])			selectivity	
membrane	N_2	CH_4	CO_2	CO_2/CH_4	CO_2/N_2
PIM-300−2.0d[b]	96	73	4000	54.8	41.7
Mixed Gas (CO_2/CH_4:50/50%)					
PIM-300−2.0d	--	42.9	2317	54.0	--
Mixed Gas (CO_2/N_2: 50/50%)					
PIM-300−2.0d	75.2	--	2924	--	38.9

[a]1 barrer =1 × 10^{-10}cm^3(STP)cm/cm^2 s cmHg. [b]Pure gas separation performance.

that in pure gas tests mainly ascribed to the competitive sorption in membranes.[45] Comparing the binary CO_2/CH_4 and CO_2/N_2 tests (i.e., both with the 50/50 mol % in feed) with the pure gas tests, there is an approximate 42% drop in CO_2 permeability for binary CO_2/CH_4 tests when compared to a 27% drop in CO_2/N_2 tests. This is clearly indicating a more pronounced competitive sorption in the former than the latter due to the higher condensability of CH_4 than N_2 (e.g., T_c of CH_4 is 190.6 K and T_c of N_2 is 126.2 K[4]).

Figure 7 shows gas separation performance of our cross-linked membranes in comparison with the Robeson's upper bound. It is worth noting that the gas separation performance of the original PIM-1 membrane is slightly above the upper bounds. Our synthesized PIM-1 membrane is in fact better than the most literature reported data in terms of both gas permeability and selectivity.[14−16] It is suggested that the difference in gas separation performance from the literature data is mainly caused by different film formation protocols.[12−15] When the PIM-1 film is first treated at 300 °C for 0.5 d, the gas separation performance goes along with the upper bound line, which is typically seen in most of polymeric membranes. While a longer thermal treatment time is applied, the gas separation performance goes diagonally with the upper bound line. For example, in the H_2/CH_4 upper bound plot (i.e., Figure 7a), both gas

dx.doi.org/10.1021/ma202667y | Macromolecules 2012, 45, 1427−1437

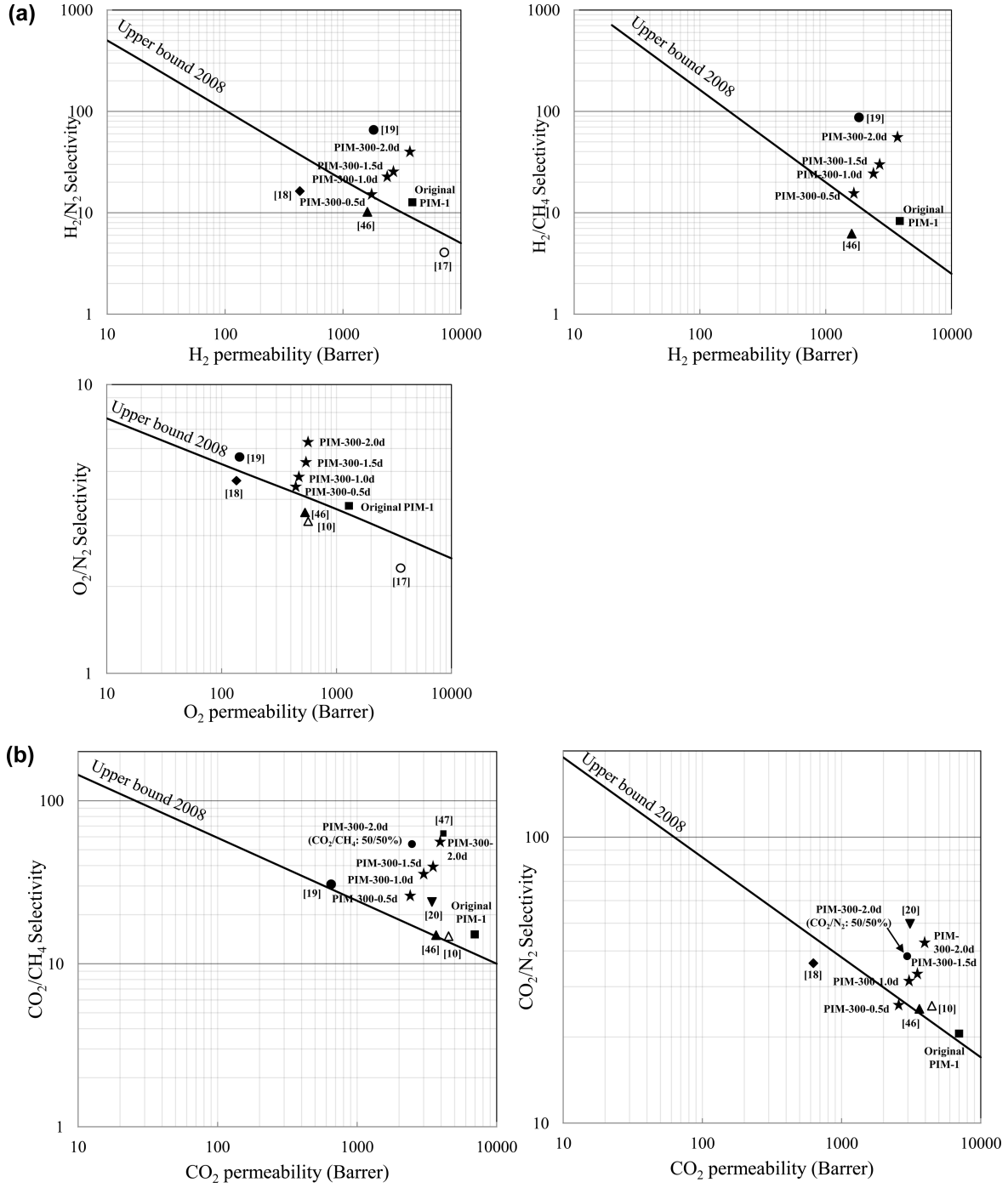

Figure 7. (a) Upper bound comparison[8] (H_2/N_2, H_2/CH_4 and O_2/N_2): PIM−PIM-8 (▲),[46] PIM-1 (Δ),[10] PIM-1/silica MMM (○),[17] carboxylated PIM-1 (♦),[18] and UV-cross-linked PIM-1 (●).[19] (b) Upper bound comparison[8] (CO_2/CH_4, and CO_2/N_2): PIM−PIM-8 (▲),[46] PIM-1 (Δ),[10] carboxylated PIM-1 (♦),[18] UV-cross-linked PIM-1 (●),[19] Tetrazole-functionalized PIM-1 (▼),[20] Thermally rearranged (TR) polymer (■).[47]

permeability and selectivity increase when PIM-1 is thermally soaked from 0.5 to 2 d at 300 °C. As discussed previously, this is resulted from a joint effect of the tightening of polymer chains and formation of bulky triazine rings. Referring to Figure 7b, the binary gas separation performance also surpasses the most recent upper bound line, which strongly suggests that the thermally cross-linked PIM-1 membranes could be used in industry gas separation. Additionally, the long-term stability test and the physical aging behavior of the selected membranes have been monitored and the results are shown in Figure 8. Compared to the original PIM-1, the thermally cross-linked membrane (i.e., PIM-300−2.0d) tends to have a better membrane stability. With consideration of the stability over a longer period, future work will be focused on physical aging over a period of at least 3 months for the thermally cross-linked membranes and ways to enhance the degree of cross-linking reaction while minimizing the thermal energy consumed.

dx.doi.org/10.1021/ma202667y | Macromolecules 2012, 45, 1427−1437

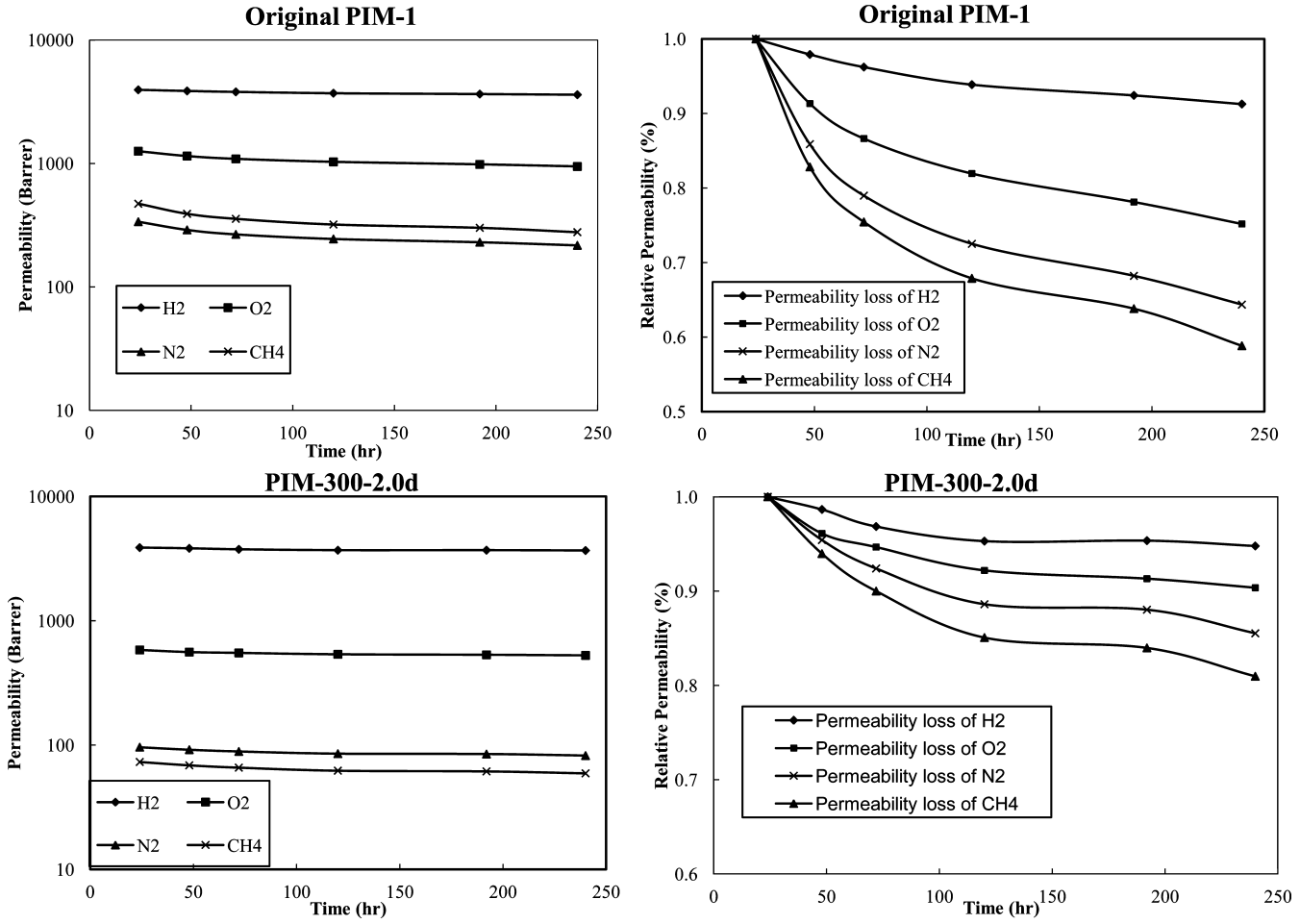

Figure 8. Aging behavior of the original and the thermally cross-linked PIM-1 membranes.

CONCLUSIONS

The high performance PIM-1 membrane has been successfully synthesized in our laboratory. The chemical structure of PIM-1 has been confirmed by XPS, FTIR and NMR analyses. After the thermal treatment of the PIM-1 film at an elevated temperature (i.e., 300 °C) for an extended period of time, the PIM-1 polymer chains tend to undergo a latent self-cross-linking reaction forming stable triazine rings. Both FTIR and XPS analyses of the resultant cross-linked PIM-1 membranes support the occurrence of cross-linking reaction and conversion of nitriles to imines. The degree of cross-linking reaction increases with an increase in thermal cross-linking time, which is also confirmed by gel content analyses. TGA analyses show an increase in thermal stability of the membrane after thermal cross-linking reaction and there is a reduction in the maximum decomposition rate when the PIM-1 membrane is thermally treated at a longer period of time. On the basis of PAL results, a clear reduction in τ_3 value with an increase in thermal treatment time suggests the chain tightening effects in the cross-linking reaction, while the formation of bulky triazine rings in the planar structure during the cross-linking reaction simultaneously constrains the polymer chains and prevents them from moving around. With the nature of the contorted structure of PIM-1 backbone, the cross-linking reaction would lead to the pronounced inefficient chain packing, thus an increase in free volume and gas permeability with the increase in thermal soaking time. In general, the thermally cross-linked PIM-1 membranes demonstrate exceptional gas separation performance that surpasses the most recent upper bounds for the important gas pairs, such as H_2/N_2, CO_2/CH_4, and CO_2/N_2. An ideal CO_2/CH_4 selectivity of 54.8, which is almost four times higher than the host PIM-1 membrane, with CO_2 permeability of 4000 barrer was obtained for PIM-1 membrane treated at 300 °C for 2 d, and mixed gas tests revealed a similar selectivity of 54. In conclusion, the thermally cross-linked PIM-1 membranes will possibly provide a promising alternative in industrial flue gas separation, natural gas purification and CO_2 capture process.

AUTHOR INFORMATION

Corresponding Author

*E-mail: chencts@nus.edu.sg.

Notes

The authors declare no competing financial interest.

ACKNOWLEDGMENTS

The authors sincerely express their gratitude to the Singapore National Research Foundation (NRF) for the financial support on the Competitive Research Programme for the project titled: "Molecular Engineering of Membrane Materials: Research and Technology for Energy Development of Hydrogen, Natural Gas and Syngas" (Grant Number R-279-000-261-281). Special thanks are also due to Miss Chua Mei Ling for her kind assistance in this work.

REFERENCES

(1) Nunes, S. P.; Peinemann, K.-V. *Membrane Technology in the Chemical Industry*; Wiley-VCH: Weinheim, Germany, 2006.
(2) Shao, L.; Samseth, J.; Hägg, M.-B. *J. Membr. Sci.* **2009**, *326*, 285−292.
(3) Car, A.; Stropnik, C.; Yave, W.; Peinemann, K.-V. *Adv. Funct. Mater.* **2008**, *18*, 2815−2823.
(4) Paul, D. R.; Yampolskii, Y. P. *Polymeric Gas Separation Membranes*; CRC Press: Boca Raton, FL, 1994.
(5) Bernardo, P.; Drioli, E.; Golemme, G. *Ind. Eng. Chem. Res.* **2009**, *48*, 4638−4663.
(6) Xiao, Y.; Chung, T. S. *Energy Environ. Sci.* **2011**, *4*, 201−208.
(7) Grainger, D.; Hägg, M.-B. *J. Membr. Sci.* **2007**, *306*, 307−317.
(8) Robeson, L. M. *J. Membr. Sci.* **2008**, *320*, 390−400.
(9) Budd, P. M.; Elabas, E. S.; Ghanem, B. S.; Makhseed, S.; McKeown, N. B.; Msayib, K. J.; Tattershall, C. E.; Wang, D. *Adv. Mater.* **2004**, *16*, 456−459.
(10) Budd, P. M.; Msayib, K. J.; Tattershall, C. E.; Ghanem, B. S.; Reynolds, K. J.; McKeown, N. B.; Fritsch, D. *J. Membr. Sci.* **2005**, *251*, 263−269.
(11) Du, N.; Song, J.; Robertson, G. P.; Pinnau, I.; Guiver, M. D. *Macromol. Rapid Commun.* **2008**, *29*, 783−788.
(12) Du, N.; Robertson, G. P.; Song, J.; Pinnau, I.; Thomas, S.; Guiver, M. D. *Macromolecules* **2008**, *41*, 9656−9662.
(13) Budd, P. M.; McKeown, N. B.; Ghanem, B. S.; Msayib, K. J.; Fritsch, D.; Starannikova, L.; Belov, N.; Sanfirova, O.; Yampolskii, Y.; Shantarovich, V. *J. Membr. Sci.* **2008**, *325*, 851−860.
(14) Staiger, C. L.; Pas, S. J.; Hill, A. J.; Cornelius, C. J. *Chem. Mater.* **2008**, *20*, 2606−2608.
(15) Song, J.; Du, N.; Dai, Y.; Roberson, G. P.; Guiver, M. D.; Thomas, S.; Pinnau, I. *Macromolecules* **2008**, *41*, 7411−7417.
(16) Thomas, S.; Pinnau, I.; Du, N.; Guiver, M. D. *J. Membr. Sci.* **2009**, *338*, 1−4.
(17) Ahn, J.; Chung, W.-J.; Pinnau, I.; Song, J.; Du, N.; Robertson, G. P.; Guiver, M. D. *J. Membr. Sci.* **2010**, *346*, 280−287.
(18) Du, N.; Robertson, G. P.; Song, J.; Pinnau, I.; Guiver, M. D. *Macromolecules* **2009**, *42*, 6038−6043.
(19) Liu, C.; Wilson, S. T.; Lesch, D. A. US Patent, 7,758,751, 2010.
(20) Du, N.; Park, H. B.; Robertson, G. P.; Dal-Cin, M. M.; Visser, T.; Scoles, L.; Guiver, M. D. *Nat. Mater.* **2011**, *10*, 372−375.
(21) Mason, C. R.; Maynard-Atem, L.; Al-Harbi, N. M.; Budd, P. M.; Bernardo, P.; Bazzarelli, F.; Clarizia, G.; Jansen, J. C. *Macromolecules* **2011**, *44*, 6471−6479.
(22) Hergenrother, P. M. *Macromolecules* **1974**, *7*, 575−582.
(23) Haddad, I. E.; Hurley, S. A.; Marvel, C. S. US Patent, 3,987,016, 1976.
(24) Idage, S. B.; Idage, B. B.; Shinde, B. M.; Vernekar, S. P. *J. Polym. Sci., Part A: Polym. Chem.* **1989**, *27*, 583−594.
(25) Mercer, F. W.; McKenzie, M. T.; Easteal, A.; Moses, S. J. *Polymer* **1994**, *35*, 5355−5363.
(26) Yu, G.; Wang, J.; Liu, C.; Lin, E.; Jian, X. *Polymer* **2009**, *50*, 1700−1708.
(27) Jean, Y. C.; Mallon, P. E.; Schrader, D. M. *Positron and Positronium Chemistry*; World Sci.: Singapore, 2003.
(28) Tao, S. J. *J. Chem. Phys.* **1972**, *56*, 5499−5510.
(29) Williams, M. L.; Landel, R. F.; Ferry, J. D. *J. Am. Chem. Soc.* **1955**, *77*, 3701−3707.
(30) Jean, Y. C. *Microchem. J.* **1990**, *42*, 72−102.
(31) Shukla, A.; Hoffmann, L.; Manuel, A. A.; Peter, M. *Mater. Sci. Forum* **1977**, *255*, 233−237.
(32) Shieh, J. J.; Chung, T. S. *J. Polym. Sci. Polym. Phys.* **1999**, *37*, 2851−2861.
(33) Tin, P. S.; Chung, T. S.; Liu, Y.; Wang, R.; Liu, S. L.; Pramoda, K. P. *J. Membr. Sci.* **2003**, *225*, 77−90.
(34) Wang, H.; Liu, S.; Chung, T. S.; Chen, H.; Jean, Y. C.; Pramoda, K. P. *Polymer* **2011**, *52*, 5127−5138.
(35) Clark, D. T. *Adv. Polym. Sci.* **1977**, *24*, 125−188.
(36) Hiraoka, H.; Lee, W.-Y. *Macromolecules* **1978**, *11*, 622−624.
(37) Rossi, F.; Andre, B.; Veen, A. V.; Mijnarends, P. E.; Schut, H.; Labohm, F.; Dunlop, H.; Delplancke, M. P.; Hubbard, K. *J. Mater. Res.* **1994**, *9*, 2440−2449.
(38) Dementjev, A. P.; de Graaf, A.; Van de Sanden, M. C. M.; Maslakov, K. I.; Naumkin, A. V.; Serov, A. A. *Diamond Relat. Mater.* **2000**, *9*, 1904−1907.
(39) Xiao, Y.; Shao, L.; Chung, T. S.; Schiraldi, D. A. *Ind. Eng. Chem. Res.* **2005**, *44*, 3059−3067.
(40) Hasegawa, M.; Kochi, M.; Mita, I.; Yokota, R. *Eur. Polym. J.* **1989**, *25*, 349−354.
(41) Tin, P. S.; Chung, T. S.; Hill, A. J. *Ind. Eng. Chem. Res.* **2004**, *43*, 6476−6483.
(42) Shao, L.; Chung, T. S.; Goh, S. H.; Pramoda, K. P. *J. Membr. Sci.* **2004**, *238*, 153−163.
(43) Du, N.; Robertson, G. P.; Pinnau, I.; Guiver, M. D. *Macromolecules* **2009**, *42*, 6023−6030.
(44) McKeown, N. B.; Budd, P. M. *Macromolecules* **2010**, *43*, 5163−5176.
(45) Coleman, M. R.; Koros, W. J. *Macromolecules* **1999**, *32*, 3106−3113.
(46) Ghanem, B. S.; McKeown, N. B.; Budd, P. M.; Selbie, J. D.; Fritsch, D. *Adv. Mater.* **2008**, *20*, 2766−2771.
(47) Park, H. B.; Jung, C. H.; Lee, Y. M.; Hill, A. J.; Pas, S. J.; Mudie, S. T.; Wagner, E. V.; Freeman, B. D.; Cookson, D. J. *Science* **2007**, *318*, 254−258.